STOCHASTIC RESONANCE: THE ROLE OF α-STABLE NOISES*

B. Dybiec†, E. Gudowska-Nowak‡

Marian Smoluchowski Institute of Physics, Jagellonian University
and
Mark Kac Complex Systems Research Center
Reymonta 4, 30–059 Kraków, Poland

(Received February 28, 2006)

Dedicated to Professor Peter Talkner on the occasion of his 60th birthday

In order to document and discuss the widespread presence in nature of the stochastic resonance phenomenon (SR), we investigate the generic double-well potential model perturbed by the α-stable Lévy type noises. Despite possible infinite variance characteristics of the noise term, the SR effect still occurs and can be detected by common quantifiers used in the studies of the phenomenon. The robustness of the SR is examined by use of standard measures within a continuous and a two-state description of the system. Since the α-stable noises are characterized by a whole set of parameters, our research focuses on the analysis of the influence of noise parameters on a shape of the signal-to-noise ratio and spectral power amplification curves, revealing presence of the SR in the system at hand. Examination of the driving noise asymmetry indicates that the resonant response weakens when the symmetric noises with a decreasing value of the stability index α are applied.

PACS numbers: 05.90.–m, 05.40.–a, 02.50.–r, 82.20.–w

1. Introduction

Stochastic resonance [1–7] is one of the phenomena manifesting a counter-intuitive, constructive role of noises in nonequilibrium physical systems. In particular, in the regime commonly named as stochastic resonant response

* Presented at the XVIII Marian Smoluchowski Symposium on Statistical Physics, Zakopane, Poland, September 3–6, 2005.

† bartek@th.if.uj.edu.pl
‡ gudowska@th.if.uj.edu.pl

of a system when appropriately tuning the intensity of a superimposed noise, the amplification and the improvement of an input, information signal are detected. The effect can be determined by use of various system performance measures, such as the signal-to-noise ratio (SNR), the spectral power amplification (SPA) or input/output cross-correlation measures. All these parameters, at a certain optimal noise level, exhibit a marked maximum. Likewise, an entropy-based measure of disorder attains a minimum thus providing a further proof for the noise-induced ordering.

The term "stochastic resonance" was introduced in the early papers addressing periodic recurrences of the Earth's ice ages for which a bistable oscillator model was proposed [8,9]. Besides, the SR phenomenon was experimentally observed in digital devices such as Schmitt triggers [10,11] and physical systems such as ring lasers [12], vertical cavity, surface emitting lasers [13] or colloidal systems [14]. Characteristic features of the SR-type response were also found in chemical reactions [15] and biological systems [16–19].

Almost all research studies devoted to the SR phenomenon were treating the input noise processes as solely Gaussian and hence, had finite variance. Instead, in this article we focus on the theoretical examination of the SR in a generic double-well potential system subjected to more general stochastic drivings: The common additive Gaussian fluctuations are replaced with an α-stable white noise, which for certain sets of parameters is equivalent to its standard, Gaussian white-noise analogue. In this respect, studies of the system perturbed by α-stable white noises reproduce the results of Gaussian models as a special case. In overall, our simulations prove that the SR effect can be observable also in systems driven by a feedback resulting from the infinite-variance noises.

2. Model

As a starting point for the examination of the influence of Lévy stable noises on the character of the SR, we chose an (overdamped) Langevin equation

$$\frac{dx(t)}{dt} = -V'(x,t) + \zeta(t) = f(x) + i(t) + \zeta(t)\,, \tag{1}$$

where $V(x,t)$ is a double-well potential with a periodically changing relative depth of its minima (*cf.* Fig. 1)

$$V(x,t) = -\frac{a}{2}x^2 + \frac{b}{4}x^4 - A_0 x \cos \Omega t\,, \tag{2}$$

with $b = 512,\ a = 128,\ A_0 = 8$. Such a choice of the potential parameters results in a sufficiently high potential barrier. Here $\zeta(t)$ stands for a white Lévy process [20]. In the above formulation $i(t) = A_0 \cos \Omega t$ represents the signal process forcing the dynamical system $\dot{x}(t) = f(x)$ perturbed by a noise term $\zeta(t)$. The proposed model is studied via the Monte Carlo simulation of the discretised Langevin dynamics [21]. The integration of Eq. (1) is performed with respect to the Lévy stable motion [21, 22] according to the recipe given by Eq. (5).

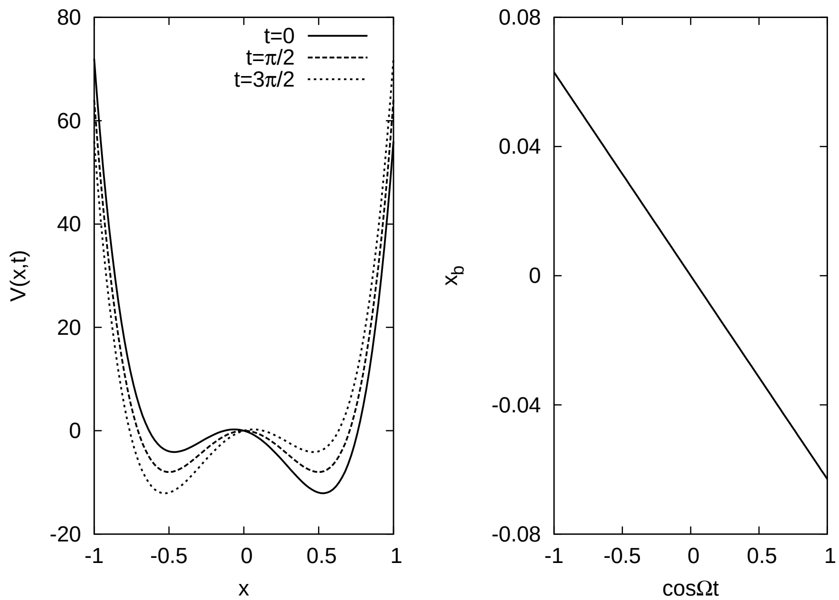

Fig. 1. The generic double-well potential (left panel) $V(x,t) = -\frac{a}{2}x^2 + \frac{b}{4}x^4 - A_0 x \cos \Omega t$ with $a = 512,\ b = 128,\ A_0 = 8$ for $t = \{0, \pi/2, 3\pi/2\}$. Note that location of the top of the potential barrier (right panel) is a function of the $\cos \Omega t$. The preferable direction of the motion in the presence of a non-biased (symmetric) noise is from a shallower — to a deeper minimum. The position of the top of the barrier is used to discriminate between "left" and "right" states of the process, *i.e.* the continuous trajectory of a "test" particle is mapped onto a two state process.

3. Solution and results

The α-stable variables are random variables for which the sum of random variables is distributed according to the same distribution as each variable [23], *i.e.*

$$aX_1 + bX_2 \stackrel{\mathrm{d}}{=} cX + d\,. \tag{3}$$

The equality $\stackrel{\mathrm{d}}{=}$ reads "equality in distribution", *i.e.* it indicates that characteristic functions of LHS and RHS of Eq. (3) are the same for a given set a, b, c, d of real numbers.

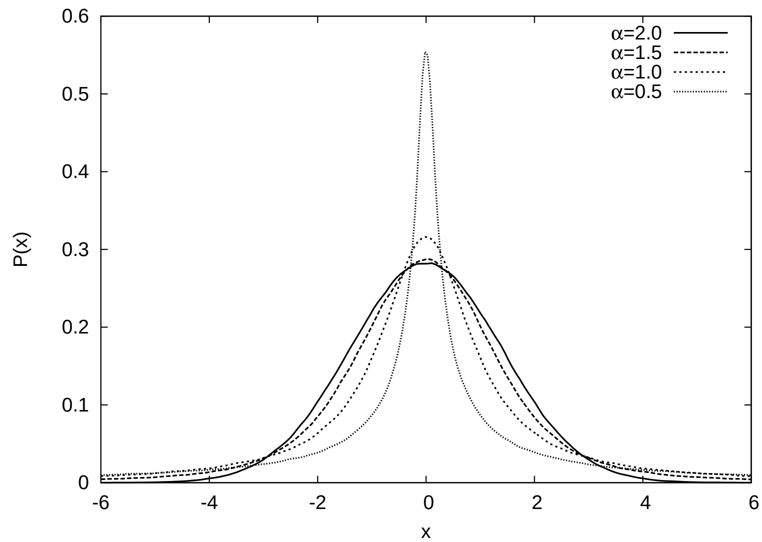

Fig. 2. Probability density functions for the symmetric ($\beta = 0$) stable random variables with an index $\alpha = 2.0, 1.5, 1.0, 0.5$ (from bottom to top). With the decreasing stability index α distributions' tails become heavier.

Accordingly, the noise term in Eq. (1) is composed of independent differential increments that follow the stable density with the index α, $L_{\alpha,\beta}(\zeta;\sigma,\mu)$. Throughout the paper we adhere to one of possible parameterizations of α-stable distributions [22, 24] which allows to write down the characteristic function of an appropriate probability distribution

$$\phi(k) = \int_{-\infty}^{\infty} e^{-ik\zeta} L_{\alpha,\beta}(\zeta;\sigma,\mu) d\zeta$$

in the form of

$$\begin{aligned} \phi(k) &= \exp\left[-\sigma^\alpha |k|^\alpha \left(1 - i\beta \mathrm{sign}(k) \tan\frac{\pi\alpha}{2}\right) + i\mu k\right], \\ \phi(k) &= \exp\left[-\sigma|k| \left(1 + i\beta\frac{2}{\pi}\mathrm{sign}(k)\ln|k|\right) + i\mu k\right], \end{aligned} \qquad (4)$$

for $\alpha \neq 1$ (upper line) and $\alpha = 1$ (bottom line), respectively. Here α stands for the stability index that describes an asymptotic power law of the ζ-distribution, $L_{\alpha,\beta}(\zeta) \sim |\zeta|^{-(\alpha+1)}$ and covers the regime $\alpha \in (0, 2]$. The parameter β represents skewness of the distribution ($\beta \in [-1, 1]$), σ characterizes a scale and μ denotes the location parameter [22, 24]. Closed, analytical forms of the probability density function (PDF) for stable variables are known only in few cases. In particular, for $\alpha = 2, \beta = 0$, ζ is a Gaussian variable, whereas $\alpha = 1, \beta = 0$ and $\alpha = \frac{1}{2}, \beta = 1$ yield Cauchy and Lévy–Smirnoff ($\zeta > \mu$) distributions, respectively. Exemplary stable probability density functions are presented in Figs. 2 and 3.

The position of a "test" particle, moving according to Eq. (1) can be obtained by direct integration [22, 25–27] yielding

$$
\begin{aligned}
x(t) \; &= \; -\int\limits_{t_0}^{t} V'(x(s),s)ds + \int\limits_{t_0}^{t} dL_{\alpha,\beta}(s) \\
&\stackrel{\mathrm{d}}{=} \; -\int\limits_{t_0}^{t} V'((x(s),s))ds + \sum_{i=0}^{N-1} (\Delta s)^{1/\alpha} \varsigma_i \, . \qquad (5)
\end{aligned}
$$

where ς_i are independent identically distributed random variables distributed according to $L_{\alpha,\beta}(\varsigma; \sigma, \mu = 0)$ and $N\Delta s = t - t_0$.

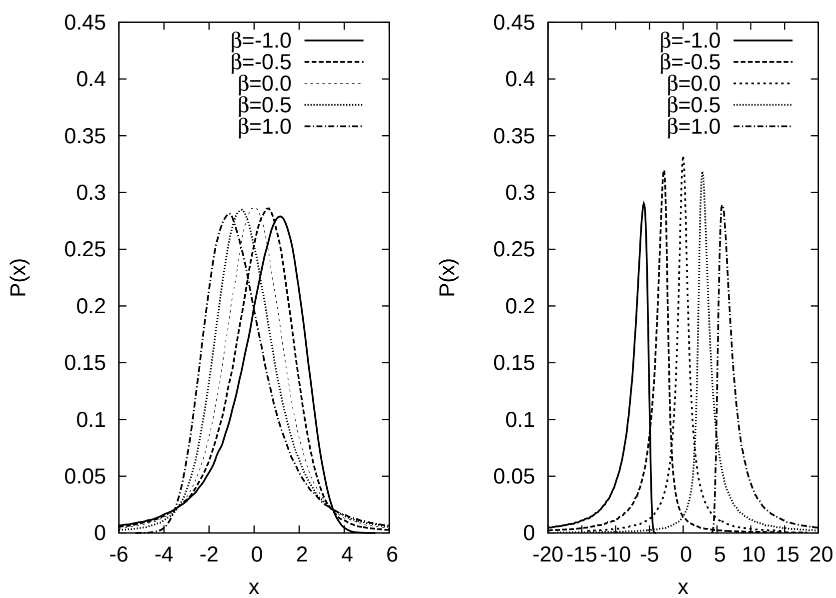

Fig. 3. Asymmetric stable probability density functions for $\beta = -1.0, \; -0.5, 0.0, 0.5, 1.0$ with $\alpha = 1.5$ (left panel) and $\alpha = 0.9$ (right panel). Note the differences in the position of the maxima for $\alpha < 1$ and $\alpha > 1$. The support of the densities for the fully asymmetric cases with $\beta = \pm 1$ and $\alpha < 1$ assumes only negative values for $\beta = -1$ and only positive values for $\beta = +1$.

Random variables ς corresponding to the characteristic function (4) can be generated using the Janicki–Weron algorithm [22]. For $\alpha \neq 1$ their representation is

$$\varsigma = D_{\alpha,\beta,\sigma}\frac{\sin(\alpha(V+C_{\alpha,\beta}))}{(\cos(V))^{1/\alpha}}\left[\frac{\cos(V-\alpha(V+C_{\alpha,\beta}))}{W}\right]^{(1-\alpha)/\alpha}+\mu, \quad (6)$$

with constants C, D given by

$$C_{\alpha,\beta}=\frac{\arctan\left(\beta\tan\left(\frac{\pi\alpha}{2}\right)\right)}{\alpha}, \quad D_{\alpha,\beta,\sigma}=\sigma\left[\cos\left(\arctan\left(\beta\tan\left(\frac{\pi\alpha}{2}\right)\right)\right)\right]^{-1/\alpha}. \quad (7)$$

For $\alpha = 1$, ς can be obtained from the formula

$$\varsigma = \frac{2\sigma}{\pi}\left[\left(\frac{\pi}{2}+\beta V\right)\tan(V)-\beta\ln\left(\frac{\frac{\pi}{2}W\cos(V)}{\frac{\pi}{2}+\beta V}\right)\right]+\mu. \quad (8)$$

V is a random variable uniformly distributed over $(-\frac{\pi}{2},\frac{\pi}{2})$, W is a random variable exponentially distributed with a unit mean; V and W are statistically independent [22, 28–30].

For the stability index $\alpha = 2$, the problem described by Eq. (1) and its equivalent integral Eq. (5) correspond to the Gaussian white noise [31] scenario. In fact, numerical integration of Eq. (1) with $\alpha = 2$ reconstructed all well known results for formerly solved Gaussian cases [2, 32, 33]. Within these studies, we use instead a class of strictly stable distributions of symmetric ($\beta = 0$) and asymmetric ($\beta \neq 0$) α-stable noises for which the value of the location parameter μ was set to 0.

To quantify the SR phenomenon we use the signal-to-noise ratio SNR and the spectral power amplification SPA. The SNR measure is defined as a ratio of a spectral content of the signal $i(t)$ in the forced system to the spectral content of the noise $\zeta(t)$:

$$\mathrm{SNR}=2\left[\lim_{\Delta\omega\to 0}\int_{\Omega-\Delta\omega}^{\Omega+\Delta\omega}S(\omega)d\omega\right]\Big/ S_N(\Omega). \quad (9)$$

Here

$$\int_{\Omega-\Delta\omega}^{\Omega+\Delta\omega}S(\omega)d\omega \quad (10)$$

represents the power carried by the signal, while $S_N(\Omega)$ estimates the background noise level. In turn, the spectral power amplification (SPA) is given by the ratio of the power of the driven oscillations to that of the driving

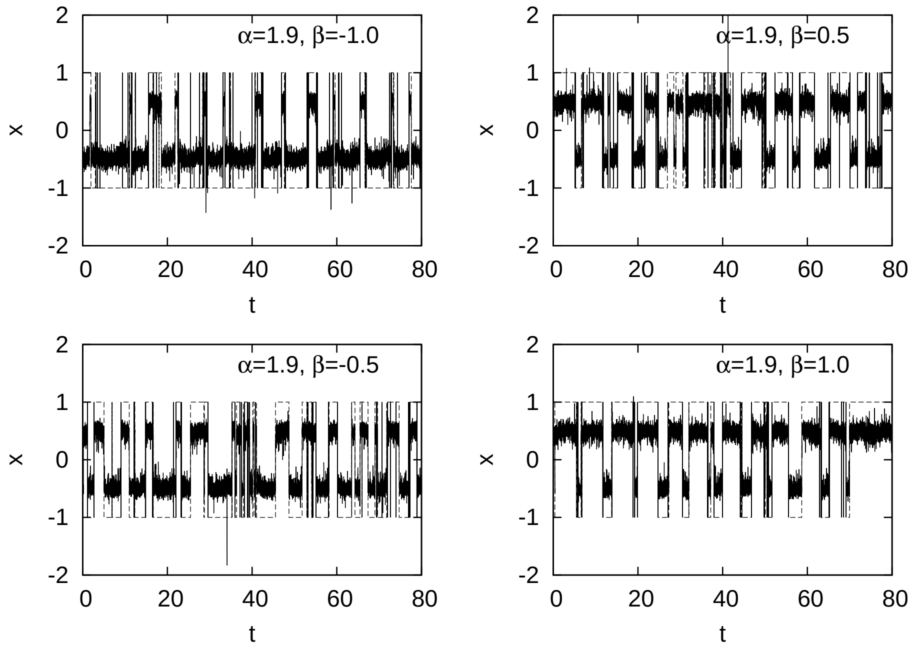

Fig. 4. Trajectories of an exemplary α-stable processes constructed by use of Eq. (1) for a two-state approximation and for the full, continuous case. The two-state process takes values ± 1. The time step of the integration is set to $\Delta t = 10^{-5}$, the scale parameter $\sigma = \sqrt{2}$. The frequency of a cycling voltage $\Omega = 1$. Noise parameters were chosen to examine possible effects coming from a skewness (bias) of the noise (see the text and *cf.* Fig. 3).

signal at the driving frequencies $\pm\Omega$. Closer examination of the resonant quantifiers reveals that both SPA and SNR behave in a typical way for the continuous *cf.* Fig. 5 and for the two-state model representations *cf.* Fig. 6. The two state approximation, *cf.* Fig. 4, is obtained from a continuous trajectory $x(t)$ by means of digital filtering, *i.e.* the actual location of the top of the potential barrier is used to discriminate between left and right states of the process marked as ± 1. The spectral amplification displays a typical bell-shaped form indicating presence of the stochastic resonance in a particular regime of the "noise intensity" σ^2. For a stability index $\alpha = 1.9$, and relatively small noise intensity (*i.e.* small scale parameter σ) the signal is not well separated from the noisy background and consequently the SNR measure is negative. With an increasing noise intensity SNR becomes positive, thus indicating separation of the signal from the noise. Figs. 5 and 6 display results of the SPA and SNR estimations in case of α-stable drivings with $\alpha = 1.9$. Results are presented for a continuous- and a two-state model. For

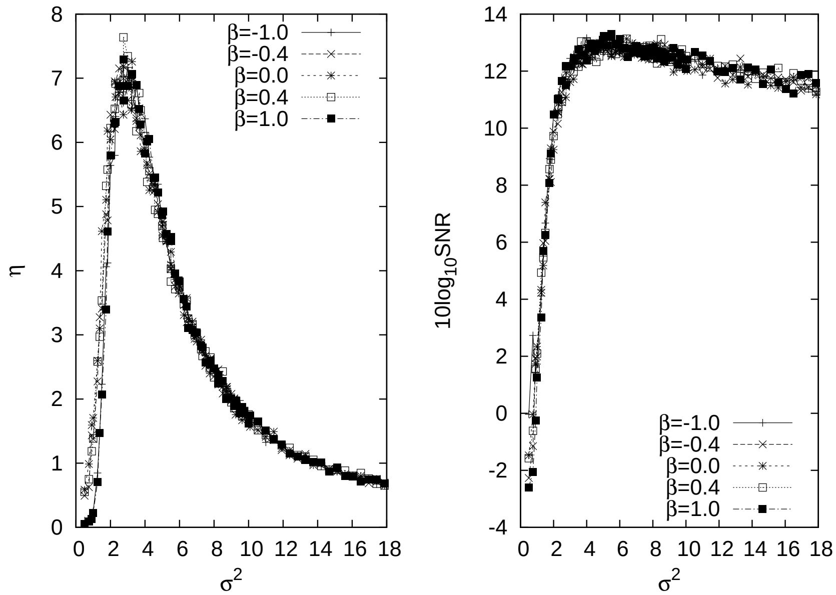

Fig. 5. SPA in arbitrary units (left panel) and SNR (right panel) for the generic potential model driven by the additive Lévy noise with $\alpha = 1.9$ and various β in the continuous approximation. The time step of the integration $\Delta t = 10^{-5}$, results were averaged over 50 realizations, $\Omega = 1$. Parameters of the potential like in Fig. 1. Lines are drawn to guide the eye only.

a given value of the stability index α the power spectra for $\pm\beta$ are the same. Therefore, stochastic resonance quantifiers derived from the power spectra are identical for $\pm\beta$ with a fixed stability index α. Exemplary trajectories of α-stable processes, corresponding to SPA and SNR from Figs. 5 and 6, are depicted in Fig. 4.

Fig. 7 reproduces trajectories of the processes driven by stable noises of higher impulsiveness, *i.e.* with the jump-length distributions characterized by progressively heavier tails ($\alpha < 2$). Note that in all these cases, the forcing noise produces jump length increments of infinite variance. Further analysis of the time-series in Fig. 7 implies that the resonant response depends on the stability index α. First of all, the decrease of α results in much larger variations and irregularity of the trajectories. Moreover, for a symmetric driving noise (left panel of Fig. 7), the decrease of α does not influence the population of the states. The latter is altered, however, by a change of the skewness parameter β (right panel of Fig. 7). The nonzero β introduces a bias, causing one of the states to be more frequently visited than the other one. This asymmetry becomes progressively stronger with a decreasing

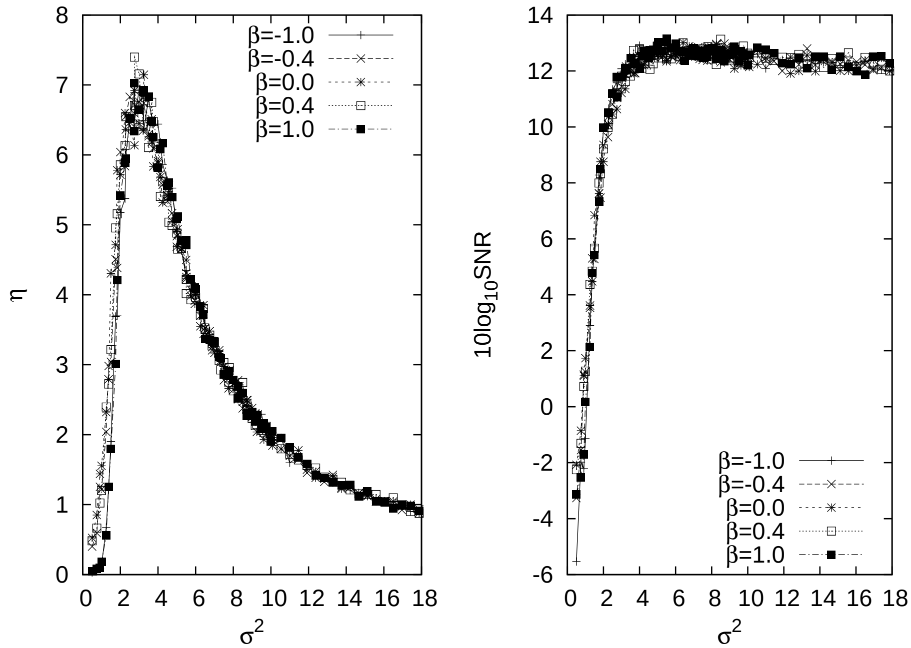

Fig. 6. The same as in Fig. 5 for the two-state model.

stability index α. Finally, for a decreasing α with $|\beta| = 1$, barrier crossing events become very rare and eventually disappear ($\alpha < 1$) due to the total skewness of the noise.

In overall, the numerical analysis presented in this work suggests that the decrease of the system performance is better visible for symmetric noises than for asymmetric ones. This effect is caused by the fact that for symmetric noises with decreasing value of the stability index α, random contribution to the particle's displacement are unbiased and increasing. Consequently, for lower value of the index α the periodic modulation of the potential barrier becomes less important for the passage problem: due to irregular random interactions of high intensity, the test particle can easily jump from one potential well to the other. Different scenario occurs, however, for skewed noises (nonzero β). The skewness of the noise favors transitions in one direction. Transitions in the opposite direction are most likely to happen when the separating potential barrier attains its minimum. Therefore, the periodicity of the signal is less disturbed by the stochastic driving with nonzero value of the skewness parameter, left *versus* right panel of Fig. 7. Moreover, the SNR measure was observed to be less sensitive to changes of the noise parameters, whereas SPA was exhibiting a pronounced decrease with lower α values (data not shown). This decrease of SPA indicates that the input

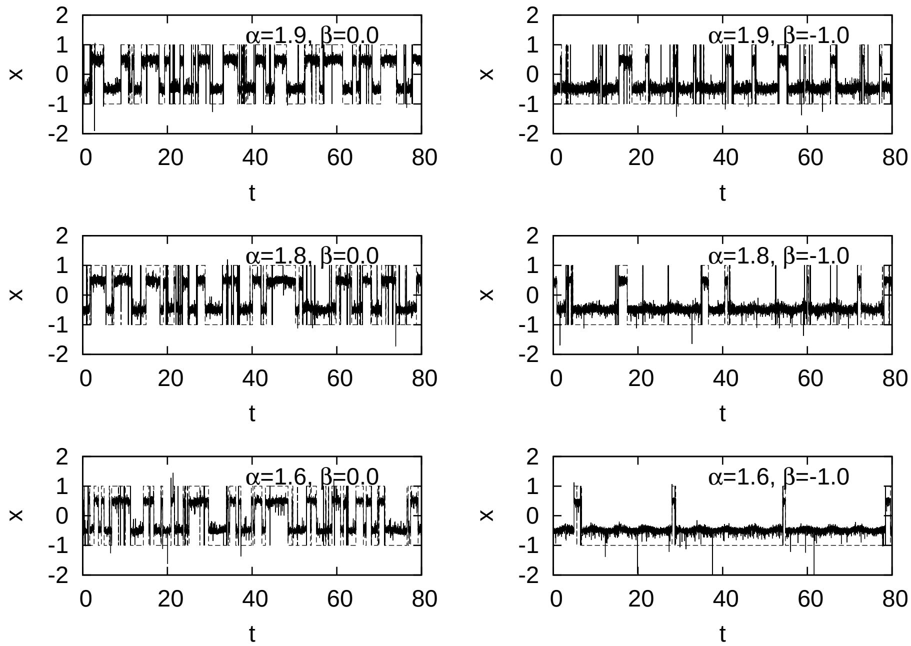

Fig. 7. Trajectories of the α-stable processes for the two-state and the continuous model constructed by use of Eq. (1). The two state process takes values ±1. The time step of the integration $\Delta t = 10^{-5}$, the scale parameter $\sigma = \sqrt{2}$. The frequency of the cycling voltage $\Omega = 1$. Noise parameters as indicated in figures.

signal becomes worse reproduced by the output signal, when the stability index is decreasing.

Similar studies were performed by other authors [34]. However, in [34] not fully correct approximation scheme to Eq. (1) was considered. Instead of $\Delta t^{1/\alpha}$ in the approximation scheme $\Delta t^{1/2}$ was taken. Nevertheless, this problem can be eliminated by proper rescaling of the parameter σ to σ' such that

$$\Delta t^{1/\alpha}\sigma' = \Delta t^{1/2}\sigma\,. \tag{11}$$

Moreover, in the work [34] an artificial constraint on allowed values of the process was imposed, *i.e.* if $|x| > 10$ then $x = 10\,\mathrm{sign}\,x$. This constraint eliminates the problem of numerical escapes of trajectories to infinity and allows integration of Eq. (1) with any time step of the integration [35].

4. Summary and conclusions

We addressed the problem of the stochastic resonance occurring in a nonlinear system coupled to a non-Gaussian noise source. The performance of the generic model based on a quartic bistable potential perturbed by a cycling, periodic forcing was examined under the influence of various types of stochastic α-stable drivings.

The system response was measured by inspection of the signal-to-noise ratio SNR and the spectral power amplification SPA. Behavior of the SR quantifiers was typical, *i.e.* it was possible to find such a value of the noise intensity, σ, for which the SR phenomenon was observed. Decrease in stability index α resulted in larger fluctuation of the output signal process $x(t)$ and consequently, caused weakening of SR. The SPA measure was detected to be more sensitive to changes in α than SNR. The larger decrease in system response was observed for symmetric, non-biased noises. In case of asymmetric noise perturbations, the SR phenomenon was more robust to decreasing values of α. Due to symmetry of the system, results constructed for given value of the stability index α were the same for $\pm\beta$. The asymmetry of the driving noise was shown to influence the population of left/right states. In conclusion, the SR effect was shown to be a robust phenomenon emerging even for the infinite-variance noise sources. More detailed analysis of the phenomenon will be presented elsewhere [36].

The Authors were supported by Polish State Committee for Scientific Research (KBN) grants 1P03B06626 (2004–2005) and 2P03B08225 (2003–2006). B.D. acknowledges the financial support from the Foundation for Polish Science through the Domestic Grant for Young Scientists (2005).

REFERENCES

[1] P. Jung, *Phys. Rep.* **234**, 175 (1993).

[2] L. Gammaitoni, F. Marchesoni, S. Santucci, *Phys. Rev. Lett.* **74**, 1052 (1995).

[3] P. Talkner, Ł. Machura, M. Schindler, P. Hänggi, J. Łuczka, *New J. Phys.* **7**, 14 (2005).

[4] L. Gammaitoni, P. Hänggi, P. Jung, F. Marchesoni, *Rev. Mod. Phys.* **70**, 223 (1998).

[5] V.S. Anishchenko, A.B. Neiman, F. Moss, L. Schimansky-Geier, *Physics–Uspekhi* **42**, 7 (1992).

[6] P. Talkner, *New J. Phys.* **1**, 4 (1999).

[7] F. Marchesoni, L. Gammaitoni, F. Apostolico, S. Santucci, *Phys. Rev.* **E62**, 146 (2000).

[8] R. Benzi, A. Sutera, A. Vulpiani, *J. Phys. A.* **14**, L453 (1981).

[9] C. Nicolis, *Tellus* **34**, 1 (1982).

[10] S. Fauve and F. Heslot, *Phys. Lett.* **A97**, 5 (1983).

[11] V.S. Anishchenko, A.B. Neiman, in *Stochastic Dynamics*, eds. L. Schimansky-Geier, T. Pöshel, Springer Verlag, Berlin 1997, p. 155.

[12] B. McNamara, K. Wiesenfeld, R. Roy, *Phys. Rev. Lett.* **60**, 2626 (1988).

[13] G. Giacomelli, F. Marin, I. Rabbiosi, *Phys. Rev. Lett.* **82**, 675 (1999).

[14] D. Babič, C. Schmitt, I. Poberaj, C. Bechinger, *Europhys. Lett.* **67**, 158 (2004).

[15] D.S. Leonard, L.E. Reichl, *Phys. Rev.* **E49**, 1734 (1994).

[16] S. Bezrukov, I. Vodyanoy, *Nature* **385**, 319 (1995).

[17] A. Fuliński, *Phys. Lett.* **A193**, 267 (1994).

[18] P. Hänggi, *Chem. Phys. Chem.* **3**, 285 (2002).

[19] P. Hänggi, G. Schmid, I. Goychuk, *Nova Acta Leopoldina* **88**, 17 (2003).

[20] A.V. Chechkin, V.Yu. Gonchar, J. Klafter, R. Metzler, L.V. Tanatarov, *J. Stat. Phys.* **115**, 1505 (2004).

[21] A. Janicki, A. Izydorczyk, *Computer Methods in Stochastic Modelling* (in Polish) Wydawnictwa Naukowo Techniczne, Warszawa 2001.

[22] A. Janicki, A. Weron, *Simulation and Chaotic Behavior of α-Stable Stochastic Processes*, Marcel Dekker, New York 1994.

[23] W. Feller, *An Introduction to Probability Theory and Its Applications*, John Wiley, New York 1968.

[24] J.P. Nolan, *Stable Distributions*, Birkhäuser, Boston 2002.

[25] B. Dybiec, E. Gudowska-Nowak, *Phys. Rev.* **E69**, 016105 (2004).

[26] B. Dybiec, E. Gudowska-Nowak, *Fluct. and Noise Lett.* **4**, L273 (2004).

[27] B. Dybiec, E. Gudowska-Nowak, *Proc. SPIE* **5467**, 411 (2004).

[28] A. Weron, R. Weron, *Lecture Notes in Physics* **457**, 379 (1995).

[29] R. Weron, *Statist. Prob. Lett.* **28**, 165 (1996).

[30] R. Weron, *Research Report HSC Wroclaw University of Technology* **1**, 1 (1996).

[31] D.J. Higham, *SIAM Rev.* **43**, 525 (2001).

[32] B. Dybiec, E. Gudowska-Nowak, *Phys. Rev.* **E66**, 026123 (2002).

[33] B. Dybiec, E. Gudowska-Nowak, P.F. Góra, *Int. J. Mod. Phys.* **C13**, 1211 (2002).

[34] B. Kosko, S. Mitaim, *Phys. Rev.* **E64**, 051110 (2001).

[35] B. Dybiec, *Stochastic Resonant Effects in System Driven by Stable Noises* (PhD Dissertation, Jagellonian University, Kraków 2005).

[36] B. Dybiec, E. Gudowska-Nowak, *Stochastic resonance in the bistable system driven by Lévy noises* (work in progress).